

Constraining the high redshift formation of black hole seeds in nuclear star clusters with gas inflows

A. Lupi^{1*}, M. Colpi², B. Devecchi, G. Galanti¹, and M. Volonteri³

¹*DiSAT, Università degli Studi dell'Insubria, Via Valleggio 11, I-22100 Como, Italy*

²*INFN, Sezione di Milano Bicocca, Piazza della Scienza 3, I-20126 Milano, Italy*

³*Institut d'Astrophysique de Paris, 98bis Bd. Arago, 75014, Paris, France*

Accepted 2014 June 4

ABSTRACT

In this paper we explore a possible route of black hole seed formation that appeal to a model by Davies, Miller & Bellovary who considered the case of the dynamical collapse of a dense cluster of stellar black holes subjected to an inflow of gas. Here, we explore this case in a broad cosmological context. The working hypotheses are that (i) nuclear star clusters form at high redshifts in pre-galactic discs hosted in dark matter halos, providing a suitable environment for the formation of stellar black holes in their cores, (ii) major central inflows of gas occur onto these clusters due to instabilities seeded in the growing discs and/or to mergers with other gas-rich halos, and that (iii) following the inflow, stellar black holes in the core avoid ejection due to the steepening to the potential well, leading to core collapse and the formation of a massive seed of $\lesssim 1000 M_{\odot}$. We simulate a cosmological box tracing the build up of the dark matter halos and there embedded baryons, and explore cluster evolution with a semi-analytical model. We show that this route is feasible, peaks at redshifts $z \lesssim 10$ and occurs in concomitance with the formation of seeds from other channels. The channel is competitive relative to others, and is independent of the metal content of the parent cluster. This mechanism of gas driven core collapse requires inflows with masses at least ten times larger than the mass of the parent star cluster, occurring on timescales shorter than the evaporation/ejection time of the stellar black holes from the core. In this respect, the results provide upper limit to the frequency of this process.

Key words: stars: black holes - black hole physics - galaxies: formation - galaxies: evolution.

1 INTRODUCTION

Observations of high redshift quasars show that black holes as massive as $\gtrsim 10^9 M_{\odot}$ were already in place at redshift $z \lesssim 7$ (Mortlock et al. 2011) when the universe was only eight hundred million years old. It is thus challenging to understand how these black holes formed when the Universe was less than 1 Gyr old and galaxies were in the process of forming.

Current models suggest that supermassive black holes may have formed from *seeds* of yet unknown mass which later grew via sustained accretion at critical or super-critical rates, and via mergers with other black holes during the hierarchical assembly of their host halos (Volonteri 2010). The origin and nature of this seed population(s) remain uncertain as uncertain are the physical mechanisms at play. This

has led to speculate that black hole seeds had masses in a wide range, between $100 M_{\odot}$ - $10^6 M_{\odot}$. To ensure early formation, seed black holes must have formed in the most massive and rare halos of a given epoch which virialise and grow in the knots of the cosmic web (Di Matteo et al. 2008).

Seed black holes may have formed as early as redshift $z \sim 20$, from the core collapse of the first very massive stars ($\gtrsim 260 M_{\odot}$) formed out of pristine gas clouds fragmenting in virialized pre-galactic halos of $10^{5-6} M_{\odot}$, i.e. the Pop III stars (Haiman et al. 1996; Tegmark et al. 1997; Heger et al. 2003; Madau & Rees 2001). The lack of metals suggest a top-heavy initial mass function and thus a first generation of seed black holes of stellar origin with masses $\lesssim 10^3 M_{\odot}$ (Abel et al. 2002; Omukai & Palla 2001; Bromm et al. 2002; Bromm & Loeb 2003; Yoshida et al. 2008). But, recent studies seem to revise the initial estimates of the stellar masses to possibly much lower values of

* E-mail: alessandro.lupi@uninsubria.it

just a few tens of solar masses (Clark et al. 2011; Greif et al. 2011; Wise et al. 2012).

Heavy seeds can form at later times ($z \lesssim 12$) from the central collapse of gas in unstable proto-galactic discs of $10^{5-6} M_{\odot}$ present in heavier ($10^{7-8} M_{\odot}$) dark matter halos (Koushiappas et al. 2004; Begelman et al. 2006; Lodato & Natarajan 2006). If the angular momentum barrier and the process of fragmentation are suppressed in some of these pre-galactic structures, due to e.g. the presence of a background of UV radiation (Agarwal et al. 2012; Latif et al. 2013), the infall of gas can continue unimpeded leading to the formation of seed black holes by direct collapse. Alternatively, a non-thermally relaxed giant star can form in these halos which is able to grow a black hole (of $\lesssim 10 M_{\odot}$) in its centre (Begelman 2010; Choi et al. 2013). In this last case, subsequent super-Eddington growth of this embryo black hole continues, inside the optically thick hydrostatic envelope, called “quasi-star” (Begelman et al. 2008). Seed black holes as heavy as $10^{4-5} M_{\odot}$ can form, depending on the extent of the radiative feedback and metal content (Montero et al. 2012; Dotan et al. 2011). A further path of black hole seed formation, not constrained by limits imposed by the metallicity content, calls for gas-rich galaxy mergers which trigger huge inflows of gas on sub-parsec scales (Mayer et al. 2010). But avoiding fragmentation of the growing gas cloud due to cooling is again matter of debate (Ferrara et al. 2013).

An alternate route for seeds formation (up to $10^2 M_{\odot} - 10^3 M_{\odot}$) has been explored considering galactic discs enriched above a critical metallicity ($Z_{\text{crit}} \sim 10^{-5} Z_{\odot}$) and in which cloud fragmentation lead to ordinary Pop II star formation (Devechi & Volonteri, 2009; D09 hereon). This path considers the formation, in some halo, of a young ultra-dense nuclear star cluster (NSC, hereafter) dominated by stellar collisions and mass segregation in its centre. A very massive star forms via star-star runaway collisions in the cluster core before single stars have time to explode in supernovae. The ensuing collapse of the runaway star eventually leads to the formation of a black hole above $\gtrsim 10^{2-3} M_{\odot}$ (Portegies Zwart & McMillan 2002; Gürkan et al. 2004; Devechi & Volonteri 2009).¹ In a cosmological context, this route has been explored by D09 who considered seed formation in pre-galactic discs. It was shown that NSCs of $10^{5-6} M_{\odot}$ develop as early as $z \sim 15 - 10$ and that the first seed black holes, from runaway stars, start dominating below this redshifts, over the Pop III channel active at earlier epochs (D09, Devechi et al., 2010; Devechi et al., 2012; D10, D12 hereon, respectively).

1.1 The Gas-Induced Runaway Merger model: GIRM

None of the above mentioned mechanisms consider the formation of massive black hole seeds from the runaway merger

¹ This pathway holds in enriched, yet metal-poor star clusters (those with metallicity below $\sim 10^{-3} Z_{\odot}$), as massive metal enriched stars lose mass via intense wind during nuclear evolution leaving a lower mass black hole or a neutron star (Heger et al. 2003). Mergers of metal rich stars can also be very disruptive (Glebbeek et al. 2009).

of stellar black holes in ultra dense star clusters. This channel was studied by Quinlan & Shapiro in the late eighties and has been revisited recently by Davies et al. (2011) who introduced a variant to this model.

In Quinlan & Shapiro (1987), a very massive Newtonian cluster of compact stars (neutron stars and stellar black holes) evolves dynamically into a state of catastrophic core collapse. Under the rather extreme conditions considered by Quinlan & Shapiro (i.e. of a galactic nucleus of 10^{7-8} stars with high initial velocity dispersion $\gtrsim 1000 \text{ km s}^{-1}$) binaries of compact stars form mainly via dissipative two-body encounters under the control of gravitational wave emission, ending in their coalescence. Following unimpeded self-similar core collapse, the central density, gravitational potential and velocity dispersion rise up to a critical limit corresponding to the onset of a relativistic dynamical instability (when the gravitational redshift z_{grav} rises above ~ 0.5). A central $\gtrsim 100 M_{\odot}$ black hole forms embracing the mass of the collapsing core.

In a subsequent paper, Quinlan & Shapiro (1989) recognised that the inclusion of a realistic mass spectrum for the compact stars combined with an accurate modelling of the stellar dynamics prevents the core from reaching the high velocity dispersions requested for the onset of the relativistic dynamical collapse. Fast mass segregation by dynamical friction combined with the tendency of stars to reach equipartition of kinetic energy (i.e. lower dispersion velocities for the heavier stars), led the core to evolve into a state of declining velocity dispersion, preventing the deepening of the gravitational potential well with time up to $z_{\text{grav}} \sim 0.5$ (see e.g. figure 3 of Quinlan & Shapiro 1989). The ultimate fate of the stellar black holes left in the centre was then found very difficult to calculate and predict, within the limits imposed by the Fokker Planck approximation used to study the system.²

Quinlan & Shapiro (1987) first recognised that only in massive galactic nuclei of 10^{7-8} stars with velocity dispersions in excess of 1000 km s^{-1} , binary stars, known to act as a kinetic energy source, do not heat dynamically the cluster to halt and reverse the gravo-thermal catastrophe of the core. In lower mass systems, such as globular clusters comprising 10^{5-6} stars, recent numerical studies indicate that most of the stellar black holes born from ordinary stellar evolution, either single or in binaries, are ejected from the cluster after a few Gyrs from formation. This follows in response to close single-binary interactions which harden the black hole binaries imparting large recoil velocities, and/or to binary coalescences via gravitational wave emission for which the induced recoil velocity can largely exceed the escape speed from the cluster (Downing et al. 2011; O’Leary et al. 2006). Either a single or a binary stellar black hole or no black

² Note that in a follow up paper, Quinlan & Shapiro (1990) showed that in galactic nuclei there is the natural tendency of triggering at their centre runaway star-star collisions during the early stage of their evolution. The very massive star is then expected to collapse into a massive black hole. This channel was later re-proposed by Portegies Zwart & McMillan (2002) in the context of young and dense star clusters of lower mass after the recognition that a wide mass spectrum leads to rapid mass segregation and multiple stellar runaway collisions ending with the formation of a massive object of $100 M_{\odot}$.

hole is left at the centre, after ejection of the bulk of the population.³

Davies et al. (2011; DMB11 hereafter) reconsider this channel of runaway merging of stellar black holes in dense star clusters, in a broader context. They envisage the case of a galaxy undergoing a merger with another galaxy or the case of a large-scale gravitational instability in a galaxy which drives (in both cases) a major central inflow of gas onto a pre-existing NSC, i.e. an inflow that can even exceed the mass of the star cluster itself. In the case the in-falling gas dominates the cluster gravitational potential, the dynamical behaviour of all stars in the cluster changes in response to the inevitable gas-induced increase of the dispersion velocity. Hard binaries present in the cluster (i.e. binaries which carry a binding energy per unit mass larger than the kinetic energy per unit mass of single stars) are turned nominally into soft binaries which soften when interacting with single stars. This process has the effect of reducing the dynamical heating of the cluster, now more susceptible to the gravo-thermal collapse. The cluster, dominated by the gravity of the underlying gas, may then enter a period of core collapse: stellar mass black holes in the hardest binaries start merging via gravitational radiation reaction before heating the cluster and/or being dynamically ejected. The enhanced escape speed due to the inflow reduces the effect of black hole ejection. Eventually the black holes in the core merge in a runaway fashion. Central velocities as large as $\gtrsim 1000 \text{ km s}^{-1}$ needs to be attained following a major gas inflow (see DMB11).

The details of this model, and in particular the effect of an inflow of gas on the fate of the stellar black holes, have not been exploited yet and future dedicated numerical experiments are necessary to assess the feasibility of this route. Hereon, we will assume that this channel operates in NSC subjected to a major inflow, postponing to an incoming paper the analysis of the interaction of the gas with the stars and black holes in the cluster (Galanti et al. in preparation). As large central inflows of gas are expected to occur during the build up of pre-galactic structures, this mechanism for black hole seed formation may be relevant during the early phases of galaxy formation.

Aim of this work is at exploring whether major inflows of gas occur at the centre of pre-galactic disc hosting a NSC, to assess the cosmological relevance of this process under the hypothesis that inflows of gas drive the runaway merger of the stellar black holes in these clusters. To this purpose, we study how a population of NSCs form and evolve inside dark matter halos assembling out to redshifts as large as ~ 20 , in concordance with the Λ CDM paradigm for hierarchical structure formation. To achieve this goal, we evolve “Pinocchio” (Monaco et al. 2002), a code which follows the cosmological evolution of dark matter halos with cosmic time, and a second code by D09, D10, D12 which creates and follows the evolution of the baryonic components in the halos, using physically motivated prescriptions for disc and star formation in pre-galactic halos. D09, D10, D12 studied a scenario

of black hole seed formation that jointly account for the early formation of a population of Pop III stars with their relic black holes, and at later times of young NSCs able to grow in their core a runaway star resulting from repeated stellar collisions which is fated to become a black hole of large mass. D10 and D12 select clusters having relaxation times shorter than the evolution time of the massive stars ($\lesssim 10^6 \text{ yr}$) for this to happen.

In this paper, we modify the code in order to include the Gas Induced black hole Runaway Merger model (hereon GIRM model) which is replacing the stellar-runaway NSC channel. The aim is at determining when black hole seeds form via the GIRM, tracing self-consistently the cosmological gas inflows in galactic halos. This implies the selection of NSCs which undergo ordinary stellar evolution and are subject to major gas inflows during the cosmic assembly of structures. We note that the stellar-runaway NSC channel is complementary to the GIRM model as the latter evolves stars under ordinary conditions. Thus a comparative analysis will enable us to assess the importance of GIRM, relative to Pop III and the stellar-runaway channel, in a cosmological context. In Section 2, we describe shortly the formation and assembly of dark matter halos and their embedded NSCs, while in Section 3 we outline the input physics of the GIRM model, deferring the reader to D10 and D12 for details. Section 4 illustrates the results and Section 5 contains our conclusions.

2 DARK MATTER HALOS, GALACTIC DISCS AND THE FORMATION OF NUCLEAR STAR CLUSTERS

“Pinocchio” is a code (Monaco et al. 2002) which evolves an initial density perturbation field, on a 3D grid, using the Lagrangian Perturbation Theory in order to generate catalogues of virialized halos at different cosmic times, keeping track of the halo’s mass, position, velocity, spin parameter, and merger history. In this paper we evolve a cosmological volume of 10 Mpc in co-moving length and adopt the Λ CDM cosmology with $\Omega_{\text{baryon}} = 0.041$, $\Omega_{\text{matter}} = 0.258$, $\Omega_{\Lambda} = 0.742$, $h = 0.742$, and $n_s = 0.963$ (Dunkley et al. 2009).

In this simulation the mass resolution is of $M_{\text{h,min}} = 3 \times 10^5 M_{\odot}$ for the dark matter halos, and is computed as the total mass in the box divided by the number of elements assigned at the onset of the simulation (Monaco et al. 2002). Dark matter elements lighter than $M_{\text{h,min}}$ do not form in the box. The corresponding resolution limit for baryons is of $5 \times 10^4 M_{\odot}$ but this limit does not represent the minimum mass scale of resolution within our semi-analytical treatment of NSC formation. According to theoretical studies, halos with mass less than $M_{\text{h,min}}$ do not fulfill the conditions for star formation and fragmentation at the redshifts explored (Barkana & Loeb 2001; Tegmark et al. 1997).

In our complex scheme (here simplified in its skeleton to outline only the key steps), virialized dark matter halos, forming at any redshift, accrete baryonic gas in a fraction equal to $\Omega_{\text{baryon}}/\Omega_{\text{matter}}$. The gas, initially in virial equilibrium, cools down at a rate computed according to the available cooling channel (either molecular or atomic cooling depending on the metallicity of the gas in the halo) and

³ There are theoretical claims that stellar mass black holes are present in some globular cluster (Moody & Sigurdsson 2009) and a recent observation seems to support this view (Strader et al. 2012).

condense into the centre of the halo. The code distinguishes between metal free halos (those with metallicity $Z < Z_{\text{crit}}$, where $Z_{\text{crit}} \sim 10^{-4.87} Z_{\odot}$ is the critical metallicity for fragmentation), and halos enriched above Z_{crit} (Santoro & Shull 2006).

- In metal free conditions, typical of the first collapsing halo, the halo virial temperature is $T_{\text{vir}} < 10^4$ K, and the only available cooling channel is that of molecular hydrogen (H_2). If enough H_2 is present in the halo, gas can cool down to $T \sim 200$ K, reaching high enough densities to form a Pop III star. In the code only a single Pop III star is allowed to form in halos with $T_{\text{vir}} \gtrsim 10^3$ K (Tegmark et al. 1997) with a mass extracted from an top-heavy initial mass function extending from a minimum to a maximum mass of 10 and 300 M_{\odot} , respectively (D10).

Pop III stars can produce a strong UV flux, able to affect the thermodynamics of gas inside the halo and in the neighbouring ones. In particular, the strong Lyman-Werner flux emitted is able to photo-dissociate H_2 molecules, thus quenching molecular cooling. Formation of new zero metallicity stars is suppressed in those halos in which the H_2 dissociation rate is higher than its formation rate. In massive halos above a threshold mass self-shielding of the gas, in the denser regions, can however prevent the disruption of molecular hydrogen (Machacek et al. 2001; Madau & Rees 2001) and this is accounted for in the simulation.⁴

- In metal enriched halos (with typical virial temperatures $T_{\text{vir}} > 10^4$) gas cools down via both atomic and molecular cooling and collapses toward the halo centre. Assuming angular momentum conservation, the cool gas settles into a large-scale pre-galactic disc described as a rotationally supported self-gravitating Mestel disc. The disc keeps on growing in mass due to continuous infall of cool gas, and the progressive increase in the gas mass causes the disc to become Toomre unstable. Torques induced by self-gravity lead to a relatively fast redistribution of gas within the disc: the gas shocks and loses angular momentum thus sinking to the centre of the halo where it forms an inner disc. The inner disc develops a steeper profile than the outer unstable disc and will become the site of NSC formation. As gas flows in the inner disc, the surface density in the outer Mestel disc decreases until the Toomre parameter increases nearing the critical value for stability ($Q_{\text{crit}} \sim 2$, in the simulations considered). At this time the central infall of gas stops. The overall process self-regulates to guarantee a condition of marginal stability in the outer disc. The mass routed in the central part and forming the inner disc then corresponds to the amount necessary for the outer disc to be marginally stable. The final configuration will then be characterised by an outer disc with Mestel profile and an inner disc with a steeper density profile (with surface density scaling as $R^{-5/3}$). The physical parameters of the two nested discs are then calculated self consistently with the transition between the outer and inner discs occurring at a transition radius R_{tr} (D10).

This holds true if fragmentation of the gas, conducive to

star formation, does not take place overall in the outer disc. As reported in Lodato & Natarajan (2007) fragmentation occurs when the gravitational induced stress into the disc is larger than a critical value. In the code, fragmentation is allowed where the cooling rate exceeds the adiabatic heating rate (D09). These two conditions determine the region where star formation (SF) sets in, which can be defined introducing a characteristic radius R_{SF} . If the outer disc grows strongly unstable, widespread star formation sets in consuming part of the gas that would otherwise flow into the inner disc. In this case $R_{\text{SF}} > R_{\text{tr}}$ and a NSC forms with a radius $R_{\text{cl}} = R_{\text{tr}}$ and a mass M_{cl} which is calculated self-consistently considering that left at disposal after gas consumption. By contrast, if the outer disc remains stable against fragmentation, star formation is triggered in the inner disc, and a NSC forms with a radius corresponding to the star formation radius, i.e. $R_{\text{cl}} = R_{\text{SF}}$ and a mass equal to the total mass of the inner disc turned into stars. A flow chart describing all the processes leading to the formation of a NSC, which has been described in this section, is reported in Figure 1.

A parameter which determines the NSC mass, in the simulation, is η , controlling the extent of baryonic inflows from the outer to the inner disc. Since star formation in the outer disc reduces the amount of gas that flows in, the net inflow rate, and thus the mass of the NSC at birth, is computed as difference between the nominal inflow rate which an unstable outer disc would have and that consumed in stars. In our simulations we assume η , as defined in D10, equal to 1. As shown in D10, the net inflow rate and the mass of the NSC at birth turn out to have a weak dependence on η (see figure 2 of D10) since with increasing η more gas is consumed by extended star formation before it can reach the inner disc. The total gas mass that has flown inwards, at the end of the simulation, turned out to be slightly lower for higher values of η . The continuous inflow of gas is a key ingredient for the model under study, as the NSC after birth is invaded by repeated episodes of gas accretion, thus leading to the evolution that we will explore in the incoming sections. Hereafter, we hypothesise that gas onto the NSC acts to deepen the potential well without turning into stars.

- In our model, the physical consequences of SNaes are included, for all channels, using motivated recipes, to account for gas depletion and metal pollution. Three million years after NSC formation, it is assumed that the most massive stars explode as SNaes, primarily leading to gas evacuation at a rate correlated to the energy of the explosion. This affects the extent of gas inflows on the NSC at subsequent times, as star formation in the surroundings of the NSC is temporarily quenched. Similarly, metal pollution from SNaes is accounted for using a simple parametric prescription which correlates the SNaes rate with the rate of injection of metals. A fraction $f_{\text{metal}} = 1 - M_{\text{sh}}/M_{\text{sn}}$, with M_{sh} the gas mass removed from the halo (see DV10) and M_{sn} the total mass released by the SN, is then retained in the halo. We remark that in the explored range of metallicities, the masses of the NSC at birth turned out to depend weakly on the metal content (as shown in figure 3 of D10).

The very massive stars in the NSC are assumed to leave behind a relic population of stellar mass black holes which form a core after mass segregating. In this paper, the core

⁴ Note that in presence of a sufficiently high Lyman-Werner background, seed black holes can form via direct collapse of warm gas clouds in some halo (Agarwal et al. 2012; Latif et al. 2013). This is a path which is not considered in this scheme.

represents the site of formation of the seed black hole after the NSC has been subjected to repeated gas inflows.

- In our cosmological scenario, halos undergo mergers, and the merger history of any halo can be obtained from Pinocchio. In the code, merger prescriptions read: (a) the total, baryonic, stellar and metal masses of the new halo are computed as sum of the masses of the two progenitors; (b) if the mass ratio between the halos is less than 1/10 the spin parameter of the main progenitor is retained, otherwise a new value is computed following Bett et al. (2007); (c) the properties of the new pre-galactic disc are calculated taking into account the new mass and angular momentum, and then disc stability, eventual inflow and star formation are re-evaluated; (d) if one or both the halos host a seed black hole, different paths can be followed. In a major merger the secondary black hole (if present) is able to reach the centre of the primary, while in a minor merger it is left wandering in the new halo (Callegari et al. 2011). The code is able to describe the remnant at the end of the merger only, but it completely neglects all processes taking place during the merger events.

- NSCs start forming around redshift $z \sim 20$ when the universe is 180 Myrs old. With the code we follow their evolution down to redshift $z \sim 6$ when the universe is $\lesssim 1$ Gyr old. We then halt the simulations, since the code does not implement any accretion history important at lower redshifts (Merloni & Heinz 2013).

3 GAS INFLOWS ONTO NUCLEAR STAR CLUSTERS

In this section we first introduce the contraction parameter, describing the dynamical response of a NSC to an arbitrary inflow of gas, and later we illustrate the implementation of the new channel of black hole seed formation, in the cosmological simulation sketched in § 2.

3.1 Contraction parameter

Consider the case of a NSC at the centre of a pre-galactic disc which is subjected to an inflow of gas, due to a perturbation inside the parent halo or due to a halo-halo merger, and let M_{gas} the total gas mass involved in the inflow. What is the kinematical response of the cluster to the inflow of gas? If, in the simplest hypothesis, the gas contributes only to the deepening of the potential well, this causes a change in the orbital velocity dispersion of the stars. Assuming that stars in the cluster move on nearly circular orbits and that their angular momentum is conserved during the inflow event, we have

$$l_* = m_* \sqrt{GM(< r_0)r_0} = m_* \sqrt{G(M(< r_0) + M_{\text{gas}})r}, \quad (1)$$

where r_0 and r are the stellar radii before and after the inflow event, respectively, and $M(< r_0)$ is the stellar mass within r_0 . In response to the inflow, the new radius is

$$r/r_0 = M(< r_0)/[M(< r_0) + M_{\text{gas}}]. \quad (2)$$

This is an over-simplifying assumption not only because stars do move on rosetta, eccentric orbits in star clusters but also because no assumption has been made on how the

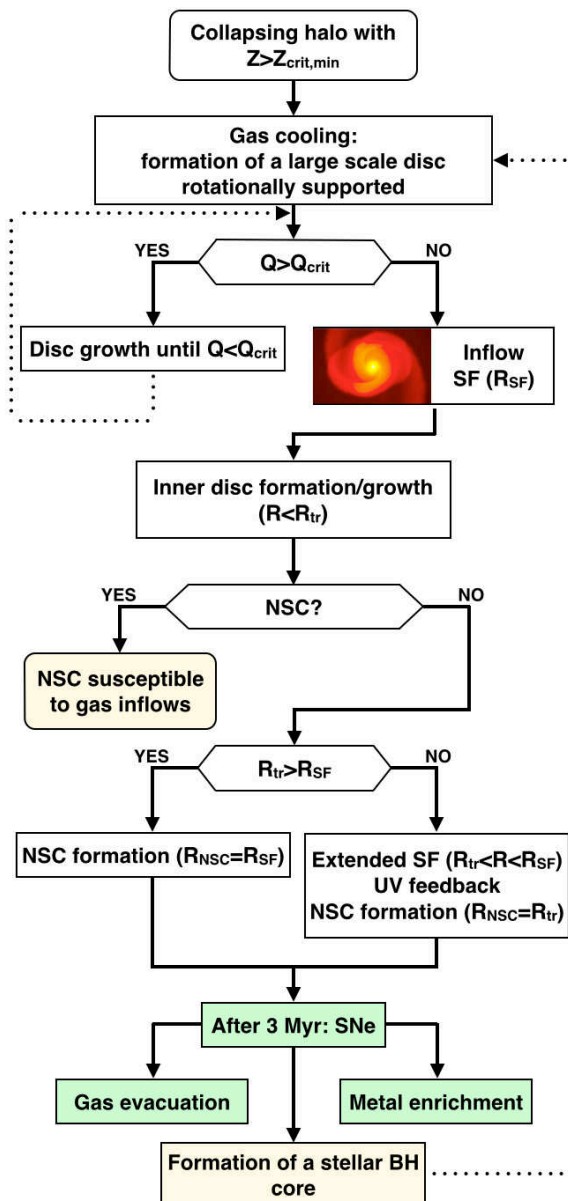


Figure 1. Flow chart of an isolated halo with $Z > Z_{\text{crit}}$, starting from gas cooling until the formation of a NSC in the centre of the halo. The processes/events in the flow chart are described in § 3.

gas is distributed inside the star’s cluster, i.e. whether is more clustered toward the centre or distributed over a much larger volume (assuming again for simplicity spherical symmetry).

In order to model different degrees of contraction for the cluster and redistribution of gas, we generalised this relation assuming a power law with a generic exponent ξ for the entire cluster, which can be written as

$$R_{\text{cl}}/R_{\text{cl},0} = [M_{\text{cl},0}/(M_{\text{cl},0} + M_{\text{gas}})]^\xi, \quad (3)$$

where R_{cl} and $R_{\text{cl},0}$ are the cluster radii before and after the inflow event. According to equation (3), $\xi = 1$.

The running value of the parameter ξ can be estimated more accurately, exploring as toy model a spherical inflow, of given mass M_{gas} , in a star cluster described by a Plum-

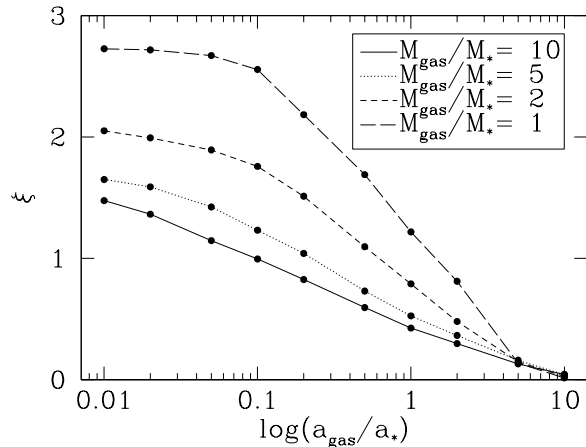
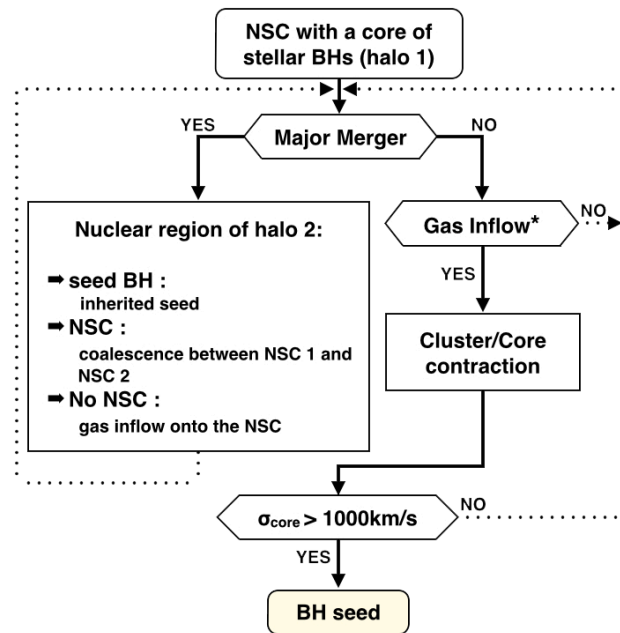


Figure 2. Contraction parameter ξ from equation (3) as a function of the ratio between the gas scale radius a_{gas} and the initial stellar scale radius a_* for different inflow masses.

mer potential of scale radius a_* initially. If during a spherical inflow, the angular momentum per unit mass of individual stars is conserved, then ξ varies between ~ 0 and ~ 3 , as illustrated in Figure 2. This figure is obtained under the assumption that also the gas after the inflow settles into virial equilibrium following a Plummer profile with scale radius a_{gas} . In Figure 2 we plot ξ as a function of a_{gas} for different values of the mass inflow M_{gas} . Varying a_{gas} is a way to mimic different cooling prescriptions for the gas which can contract down to a very small radius (in the absence of a modeling of the thermodynamical behaviour of the gas). As expected, the largest contraction occurs, for a given M_{gas} , in the limit of $a_{\text{gas}} \rightarrow 0$ and is larger the larger M_{gas} is. For a Plummer sphere, ξ saturates to a value equal to $\ln(2^{3/2}) = 2.8$ in the limit in which the whole mass M_{gas} has collapsed into a point.⁵

From this toy model we notice that cluster contraction depends on how the gas concentrates within the cluster. Since the inflow of mass on the pre-existing star cluster can occur at any time according to the evolution of the halo’s cosmic environment, and can vary from episode to episode, the contraction parameter is very susceptible to conditions that allow for a wide range of values. To bracket uncertainties we thus explore NSCs with inflows varying the contraction parameter ξ between a minimum value of 0.5 and a maximum of 3. The contraction of the star cluster due to the gas inflows also leads to an increase of the velocity dispersion of the stars which is computed according to the virial theorem, once the new radius and new total cluster’s mass are known.

⁵ The analytical estimates of ξ shown in Figure 2 match well with those obtained calculating the response of a star cluster to an external inflow, using a Monte Carlo integrator for the true dynamics of the stars (our stellar black holes) in a Plummer sphere (Galanti et al. 2014, in preparation).



*Due to minor mergers and Toomre instabilities in the outer disc

Figure 3. Flow chart reporting the NSC contraction process leading to the formation of a single seed BH from the merger among stellar mass black holes.

3.2 Modelling the Gas Induced black hole Runaway process in NSC with inflows

Let $M_{\text{cl},0}$, $R_{\text{cl},0}$ and σ_{cl} be the mass, radius and 1D velocity dispersion of the star cluster at the time of its formation. Stellar mass black holes are assumed to form after the first three Myrs and to mass segregate shortly after within a core radius $R_{\text{BH-core},0} = 0.1R_{\text{cl},0}$. The typical mass segregation timescale can be computed as

$$t_{\text{segr}} \approx \frac{\langle m_* \rangle}{m_{\text{BH}}} \frac{N}{8 \log N} \frac{R_{\text{cl},0}}{v_{*,0}}, \quad (4)$$

where $\langle m_* \rangle$ is the mean stellar mass, m_{BH} the mean black hole mass, N the number of stars and black holes in the cluster, and $v_{*,0}$ is the stellar typical velocity which can be approximated with the 1D velocity dispersion $\sigma_{\text{cl},0}$ of the cluster. If we consider a typical NSC initial mass of $10^4 M_{\odot}$, with radius $R_{\text{cl},0} = 1$ pc, mean stellar mass of $\langle m_* \rangle \simeq 1 M_{\odot}$, and $m_{\text{BH}} \sim 10 M_{\odot}$, the mass segregation timescale is ~ 4 Myr. We thus assume that a core of stellar black holes forms 4 Myr after the NSC formation. We further define $M_{\text{BH-core},0}$ as the mass in stellar black holes present in the cluster core, and $\sigma_{\text{BH-core},0}$ the black hole velocity dispersion: we assume $M_{\text{BH-core},0} = 1.5 \times 10^{-3} M_{\text{cl},0}$ ⁶ and $\sigma_{\text{BH-core}} = 26\sigma_{\text{cl}}$, where 26 corresponds to virial value $(GM_{\text{BH-core}}/R_{\text{BH-core},0})^{1/2}$.

Figure 3 shows a schematic picture of the NSC contraction process driven by gas inflow, ending with the formation of a seed black holes.

GIRM is implemented in the code as follows:

⁶ This relation is derived from $M_{\text{core},0} = m_{\text{BH}} N_{\text{BH}}$, where $N_{\text{BH}} = \alpha N_*$ with $\alpha = 0.0015$, and $M_{\text{cl},0} = \langle m_* \rangle N_* + m_{\text{BH}} N_{\text{BH}}$ (see DMB11).

- Given a mass inflow M_{gas} onto the NSC, the radius R_{cl} is updated according to equation 3, where the exponent ξ is allowed to vary between 0.5 and 3, as explained in section 3.1. The new velocity dispersion σ_{cl} is computed from the virial theorem, considering as mass the sum of the cluster and gas mass. Gas is allowed to settle into a disc of size R_{tr} , as a purely radial inflow would require an unphysical transport/cancellation of angular momentum. The gas disc has a surface density profile of the form $\Sigma_{\text{gas}} = \Sigma_0(R/R_{\text{tr}})^{-5/3}$ with $\Sigma_0 = M_{\text{gas}}/2\pi R_{\text{tr}}^2$.

- We compute the gas mass $M_{\text{gas,core}}$ enclosed in $R_{\text{BH-core}}$ from the above relation for the disc and update the stellar core radius $R_{\text{BH-core}}$ according to equation (3). The enhancement of the core velocity dispersion $\sigma_{\text{BH,core}}$ is computed from the virial relation using as mass the sum of $M_{\text{BH-core,0}}$ and $M_{\text{gas,core}}$. If, in response to an inflow, $\sigma_{\text{BH-core}}$ exceeds 1000 km s^{-1} we assume that the whole core of stellar black holes experiences GIRM, which leads to the formation of a seed of mass equal to $M_{\text{BH-core,0}}$. The choice of 1000 km s^{-1} is motivated by the study of DBM11, representing the threshold for GIRM. In the DBM11 scenario, hard binaries coalesce before experiencing single-binary encounters and, at the same time, are retained in the core as kicks from gravitational recoil are not large enough to allow black holes to escape from the cluster (having an escape speed $\sim 4000 \text{ km s}^{-1}$).

- In presence of halo-halo mergers, NSCs are modelled using simple recipes which account for the additional inflows of gas (Mihos & Hernquist). In the case of major mergers (those with mass ratio larger than 1:10) we follow these prescriptions: (a) if only one halo hosts a NSC prior to the merger, the gas of the companion halo is added to the new halo causing an inflow in the first, and the cluster and core parameters are updated considering a rapid infall. The new radius and mass of the star cluster with its embedded black hole is computed using the contraction law; (b) if both halos hosted a NSC, we merged the two into a single new cluster, and update the cluster properties following the prescriptions in Ciotti et al. (2007). Assuming that during the merger no mass is lost, energy conservation allows to estimate the virial radius R_{12} of the new cluster core of black holes as

$$\frac{1}{R_{12}} = \left(\frac{M_{\text{BH,1}} + M_{\text{g,1}}}{M_{\text{BH,12}} + M_{\text{g,12}}} \right)^2 \frac{1}{R_1} + \left(\frac{M_{\text{BH,2}} + M_{\text{g,2}}}{M_{\text{BH,12}} + M_{\text{g,12}}} \right)^2 \frac{1}{R_2}, \quad (5)$$

where $M_{\text{BH,1}}$ and $M_{\text{BH,2}}$ are the masses of the black hole cores of the progenitor clusters, $M_{\text{g,1}}$ and $M_{\text{g,2}}$ the gas masses in the cores, $M_{\text{BH,12}}$ and $M_{\text{g,12}}$ the total mass in black holes and gas of the new star clusters, respectively, and R_1 and R_2 are the virial radii of the progenitor clusters; (c) if one halo had already a seed black hole with a mass above $260 M_{\odot}$ relic of a Pop III star, this black hole is incorporated in the resulting halo as a new seed; (d) if both halos hosted a seed black hole we assumed the instantaneous coalescence of the two black holes into a more massive seed.

- In the case of minor mergers, NSCs are modelled assuming that the only change in their properties is due to an additional gas inflow. Black holes and clusters from the smaller halo are let wandering in the outer region of the resulting galaxy, and are not allowed to sink into the nuclear region (Callegari et al. 2011).

- We further explored, as ancillary study, NSCs with velocity dispersions in the interval between 40 and 100 km s^{-1} .

These NSCs have no relation with the GIRM scenario, but their presence can be easily tracked, within the cosmological scheme explored here. Their relatively high velocity dispersion (between 40 and 100 km s^{-1}) can be natal or more likely is acquired following a gas inflow. The request on the velocity enhancement here is less severe than in GIRM. This will enable us to investigate on the likelihood of an alternative scenario by Miller & Davies (2012). In this new context, NSCs with velocities dispersions in this selected range, can grow a black hole seed from a stellar mass black hole (or binary black hole). Stellar black holes, relic of massive stars, have two possible fates in these NSCs: they are either all ejected or a single (or binary) remains. The black hole (binary) which avoided ejection, can later grow via tidal captures. Dynamical arguments by Miller & Davies (2012) seem to support this picture. We thus aim to calculate the number of NSCs with velocity dispersion between 40 and 100 km s^{-1} , resulting either from the direct collapse of an unstable disc, or after a phase of gas inflow into a pre-existing cluster.

4 RESULTS

4.1 Seed black holes from GIRM in nuclear star clusters

We ran a suite of simulations, for three different values of $\xi = 0.5, 1$ and 3 for the contraction parameter. The cosmological box explored has a size of 10 Mpc and has been evolved from redshift $z \sim 40$ down to redshift $z \sim 6$, to test if the GIRM channel is able to produce a population of seed black holes large enough to explain the most massive black holes found in the Universe at redshift up to ~ 7 . We halt integration at $z \sim 6$ as our code does not include any process of accretion that can become important below this redshift.

In the simulations we considered the Pop III and GIRM channels. They are expected to contribute to the early generations of seed black holes at different cosmic epochs, as the formation of NSCs in pre-galactic discs (a necessary condition for the GIRM to operate) requires some degree of metal pollution of the intergalactic medium from the explosions of the massive Pop III stars. We remark that the GIRM channel does not pose any constraint on the level of metallicity of the parent halo, and hence on the time of formation, provided Pop III stars have enhanced the metallicity above a threshold $Z_{\text{crit}} \sim 10^{-4.87} Z_{\odot}$ (see D10-D12). The GIRM path requires the formation of ordinary star clusters and thus a population of stellar mass black holes from the core-collapse of the massive stars.

Figures 4 and 5 show the number of halos relative to the total $f_{\text{BH}} = N_{\text{BH,z}}/N_{\text{halo,z}}$ which host a newly formed black hole at any given redshift.⁷ The simulation resolution reported in the plots is computed as $1/N_{\text{halos,z}}$.

There exists an earlier epoch of black hole seed formation from Pop III, around $z \sim 20$, and a second, from the GIRM channel around $z \sim 8, 10$ and 15 according to the values of ξ (as given in Table 1), with an overlap with the Pop III channel for $\xi = 3$. A more rapid contraction of the

⁷ The case for $\xi = 1$ is intermediate between Figures 4 and 5 and is not reported for seek of simplicity.

ξ	#seed	$\langle M/M_{\odot} \rangle$	z_{peak}
0.5	405	1301.1	7.75
1.0	637	1173.4	10.0
3.0	1054	987.5	14.75
PopIII	822	70.5	27.5

Table 1. The number of black hole seeds formed from the GIRM channel (upper panel) and from Pop III (lower panel); the mean black hole seed mass and the redshift where their formation peaks, considering the three adopted values of ξ .

star cluster in response to the gas inflows (i.e. for $\xi = 3$) makes black hole formation to occur earlier and to produce a larger number of seeds. Later, the observed decline mirrors the bottom up hierarchical build up of the halos and of their embedded star clusters: less massive halos form first and require lower gas inflows to produce a seed, while heavier halos require a greater amount of gas and are less in number. In the case of $\xi = 0.5$, black hole seed formation occurs at later epochs as there is the need of a larger inflow of gas to trigger the collapse of the black hole star clusters. The decline in the Pop III channel is instead due to metal pollution from the first Pop III stars which quenches the formation of black hole seeds from pristine gas. Table 1 shows that the number of black hole seeds in the cosmological box increases with increasing ξ , and that the channel is competitive to that from Pop III. The fraction f_{BH} is larger for the Pop III channel, but with cosmic time, the absolute number of sufficiently massive dark matter halos increases so that the absolute number of natal black hole halos is larger as z decreases. The evolution of the relative contribution to the black hole seed population due to Pop III and GIRM channels is depicted in Figure 6, where we report the total seed comoving mass density as a function of redshift. In the plot the different lines correspond to the Pop III channel and GIRM channels for different values of ξ . In addition, also the total seed co-moving mass density has been represented.

As in D10, black hole seeds from PopIII stars have a typical small mass ($\sim 70 M_{\odot}$), while seeds from the GIRM channel have a larger mass, of about $\gtrsim 1000 M_{\odot}$, as the entire cluster of stellar black holes is assumed to undergo runaway merger, after a major inflow of gas. The mean mass of black holes formed via the GIRM channel decreases with increasing ξ and this can be explained with the larger fraction of NSCs with smaller masses able to core collapse before $z = 6$. In general, to form a seed the required inflow of gas is at least comparable with the mass of the target star cluster.

Figure 7 shows the black hole seed mass distribution, for the GIRM channel, for the three values of ξ , 0.5, 1, and 3. As already mentioned, the number of black hole seeds increases with increasing ξ . Despite the different mean mass, the peak of the mass distribution is around the same value of $350 M_{\odot}$, mirroring the shape of the mass distribution of the parent NSCs housing the seeds, depicted in Figure 8. The mass of the parent cluster is measured prior to the mass inflow that led to the core collapse.

In addition, Figures 9 and 10 give the total mass of the inflow (due to repeated accretion events) within the transition radius R_{tr} as a function of the black hole seed mass, evaluated when the velocity dispersion in the core reaches

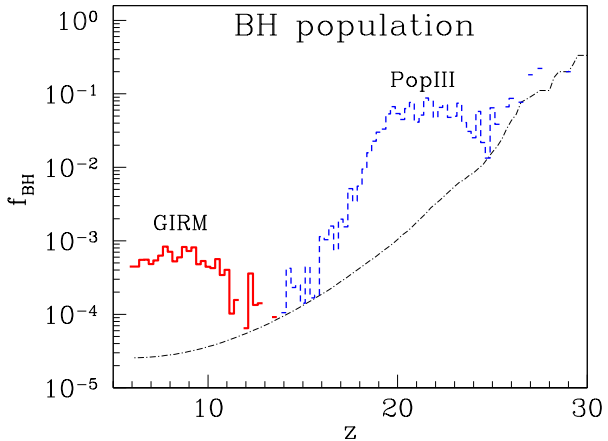


Figure 4. Fraction f_{BH} of halos hosting a newly formed seed black hole as a function of redshift, from redshift $z = 30$ down to $z = 6$. Blue line refers to the Pop III channel; red solid line refers to the fraction of black holes with mass above $260 M_{\odot}$ resulting from the GIRM channel, for a contraction parameter $\xi = 0.5$. The black dash-dotted line is the simulation resolution.

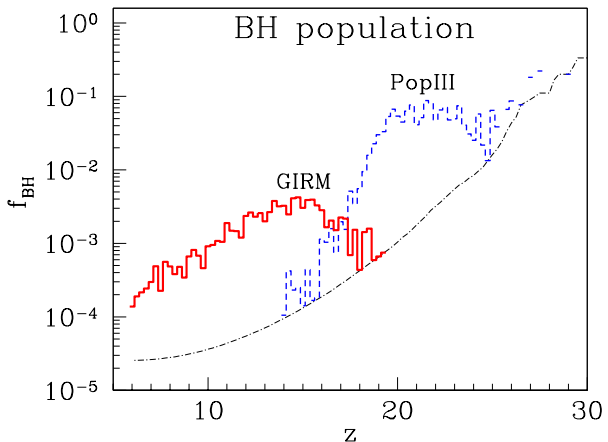


Figure 5. Fraction f_{BH} of halos hosting a newly formed seed black hole as a function of redshift, from redshift $z = 30$ down to $z = 6$. Blue line refers to the Pop III channel; red solid line refers to the fraction of black holes with mass above $260 M_{\odot}$ resulting from the GIRM channel for a contraction parameter $\xi = 3$. The black dash-dotted line is the simulation resolution.

$\sigma \gtrsim 1000 \text{ km s}^{-1}$. The red lines represent the best fit obtained assuming that $M_{\text{gas}} \propto M_{\text{BH}}$. When $\xi = 0.5$ the best line gives $M_{\text{gas}} \simeq 123 M_{\text{BH}}$, while for $\xi = 3$ we obtained $M_{\text{gas}} \simeq 870 M_{\text{BH}}$. These results show that the total inflow needed to drive the NSC core to $\sigma \gtrsim 1000 \text{ km s}^{-1}$ varies from a minimum corresponding to roughly the NSC mass up to values as large as 10 – 50 times the NSC mass.

As the extent of a gas inflow is related to the halo gas fraction and to mergers, we also expect a correlation between the total inflow needed for the GIRM to occur and the host halo mass. Combining these two relations we find that the ratio between the gas inflow mass and the seed black hole mass is almost independent of the host halo mass, as reported in Figures 11 and 12. In the case of $\xi = 0.5$ only the most massive halos ($> 3 \times 10^8 M_{\odot}$) can host a seed black hole from GIRM, while for a more efficient contraction ($\xi = 3$)

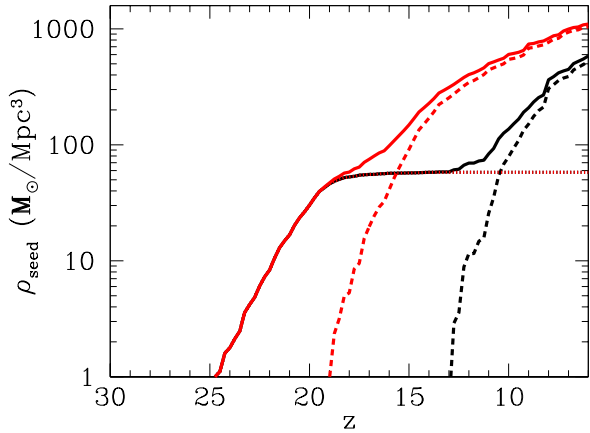


Figure 6. Black hole mass density versus redshift for the two channels. The dotted line refers to the Pop III path. The dot-dashed lines refer to the GIRM channel for $\xi = 0.5$ (right) and $\xi = 3$ (left). The total seed mass densities are also plotted with the thin solid lines, for $\xi = 0.5$ (right) and the solid one for $\xi = 3$ (left).

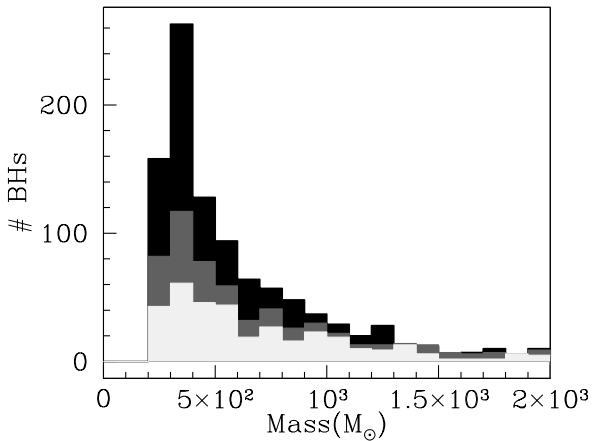


Figure 7. Mass distribution of seed black holes formed via the GIRM channel, for $\xi = 0.5$, $\xi = 1$ and $\xi = 3$. Black histogram corresponds to $\xi = 3$, grey to $\xi = 1$, and beige to $\xi = 0.5$. Black hole seeds have a typical mass of about $350 M_{\odot}$, while the mean mass, depends on the ξ , and is given in Table 1

seeds are hosted also in less massive halos. At very large halo masses the ratio varies also of two orders of magnitude, and the largest values are probably due to halos with very large inflows, overcoming the necessary threshold for GIRM to occur.

Moreover, we find that the occupation fraction of black holes F_{BH} (formed via both Pop III and GIRM channels) is a function of redshift, and it strongly depends on the host halo mass. Figures 13 and 14 show that at redshift $z = 6$ halos with masses larger than $8 - 9 \times 10^9 M_{\odot}$ host a black hole, and halos with masses lower than $2 \times 10^8 M_{\odot}$ do not at all. Note also the weak dependency on ξ of F_{BH} . For higher redshift, all the lines shift to lower masses, according to our cosmological model.

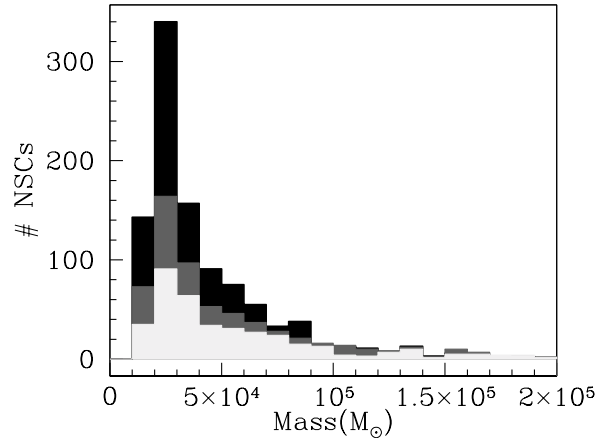


Figure 8. Mass distribution of the NSCs hosting seed black holes formed via the GIRM channel, for $\xi = 0.5, 1$, and 3 . Black histogram corresponds to $\xi = 3$, grey to $\xi = 1$, and beige to $\xi = 0.5$. The largest fraction of nuclear star clusters have a typical mass, prior to the gas inflow, of about $3.5 \cdot 10^4 M_{\odot}$.

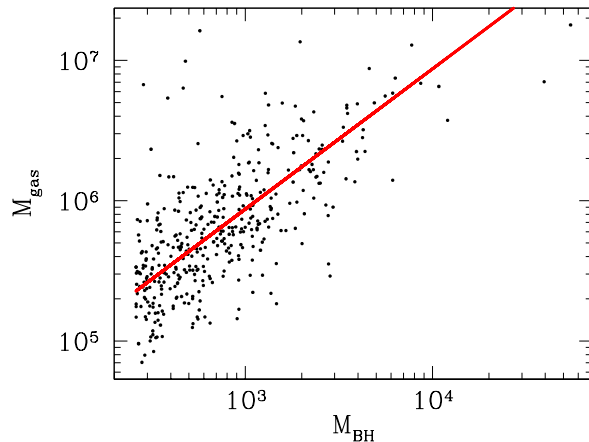


Figure 9. Gas mass resulting from inflows as a function of the seed black hole mass for the GIRM channel with $\xi = 0.5$. The red solid line corresponds to the linear fit obtained assuming a zero black hole mass for $M_{\text{gas}} = 0$.

4.2 Stellar black holes in nuclear star clusters

As anticipated in Section 2, NSCs with velocity dispersions in the interval 40 km s^{-1} and 100 km s^{-1} may be able to retain a black hole or a binary black hole of stellar mass, as suggested in Miller & Davies (2012). These clusters have gravitational potential wells deep enough, and two-body relaxation times short enough for mass segregation to lead to

ξ	$\max\{\#\text{seed}\}$	$< M_{\text{cl}}/M_{\odot} >$
0.5	4003	$5.83 \cdot 10^4$
1.0	4421	$5.22 \cdot 10^4$
3.0	4814	$4.90 \cdot 10^4$

Table 2. The number of NSC candidates for core collapse following a gas inflow or a merger, leaving a single stellar mass black hole after ejection of the black holes in the core, as discussed in Section 6, for the three different values of ξ .

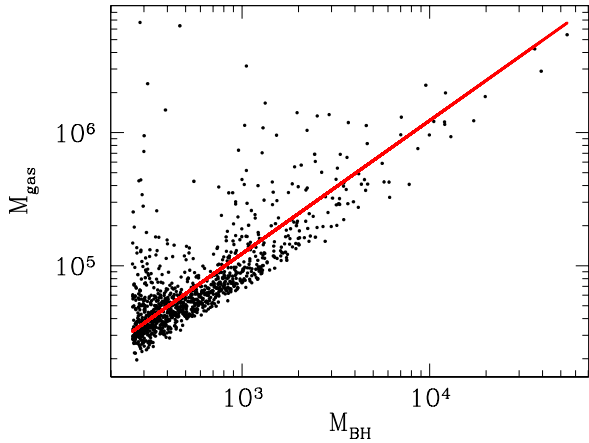


Figure 10. Gas mass resulting from inflows as a function of the seed black hole mass for the GIRM channel with $\xi = 3$. The red solid line corresponds to the linear fit obtained as in Figure 9.

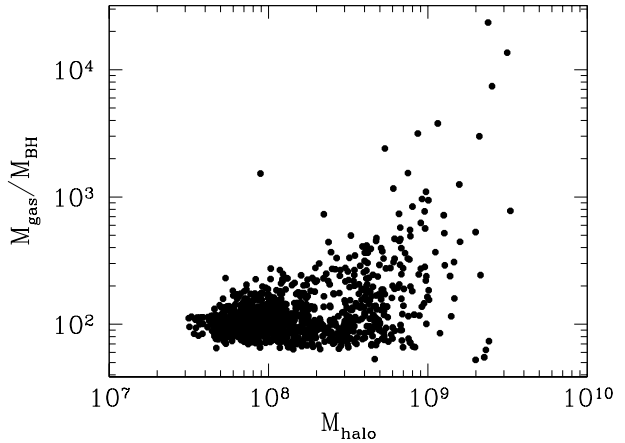


Figure 12. Gas mass to seed black hole mass ratio resulting from inflows as a function of the host halo mass for the GIRM channel with $\xi = 3$. Also in this case the ratio weakly depends on the host halo mass, except for the very large ones (same as in Figure 11).

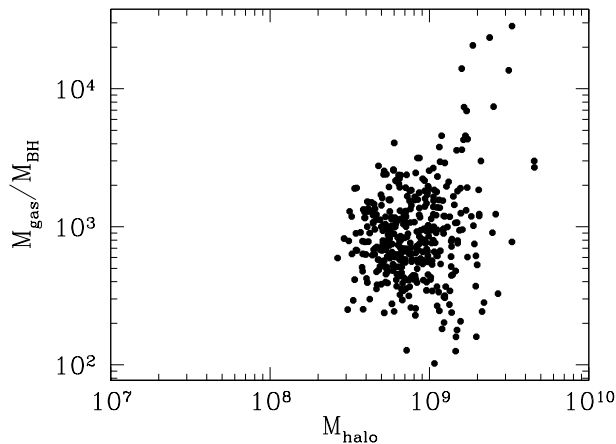


Figure 11. Gas mass to seed black hole mass ratio resulting from inflows as a function of the host halo mass for the GIRM channel with $\xi = 0.5$. The ratio is almost independent of the host halo mass, with the exception of the very large ones (where the inflow could be quite larger than that needed to GIRM) and it is almost constant with a value with an order of 10^3 .

formation of a core of stellar black holes. Having these clusters high escape speeds, black hole ejection by three-body encounters or gravitational wave recoil is incomplete and either a single stellar black hole or a black hole binary remains in the cluster which may later grow by capturing stars. Here, we briefly touch upon this model, by counting, in this subsection, the number of NSCs forming inside the pre-galactic discs that have their velocity dispersion above 40 km s^{-1} , or rise it due to a cosmological mass inflow or a merger. The results are given in Table 2 and can be considered as an upper limit to the stellar black hole population retained in these systems. The calculation indicates that at the centres of pre-galactic discs there might be the conditions to build star clusters in which an intermediate mass black hole of stellar origin can form, and this could be a further channel of formation of seeds. From a comparison between Table 1 and Table 2, we note that the number of NSCs where this

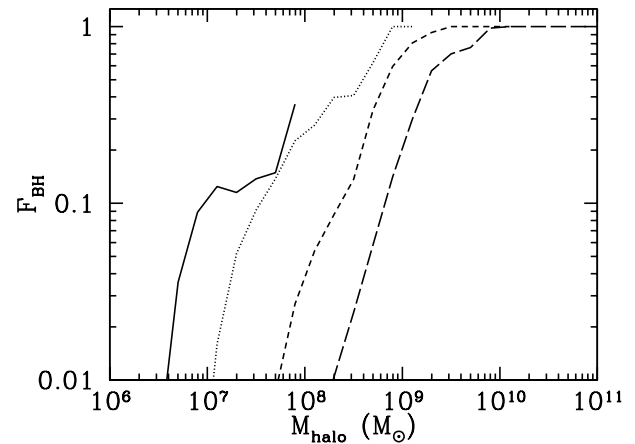


Figure 13. Occupation fraction of seed black holes versus halo mass assuming $\xi = 0.5$. From left to right the lines show values at redshift $z = 20, 15, 10, 6$, respectively.

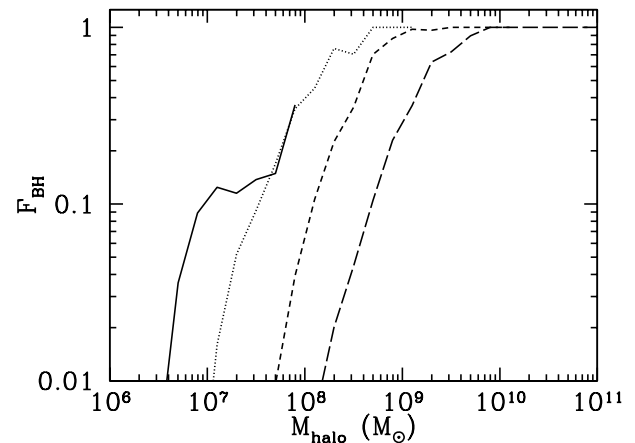


Figure 14. Occupation fraction of seed black holes versus halo mass assuming $\xi = 3$. From left to right the lines show values at redshift $z = 20, 15, 10, 6$, respectively.

scenario may happen is 4-10 higher than in the standard GIRM.

5 CONCLUSIONS

In this paper, we explored the formation of black hole seeds of $\lesssim 10^3 M_\odot$, resulting from the dynamical collapse of stellar black holes in NSCs undergoing major gas inflows, at the centre of pre-galactic discs forming at very high redshifts.

We explored the properties of this population of forming seeds combining the clustering of dark matter halos extracted from “Pinocchio” with a semi-analytical model which incorporates the physics of the inflows in a simplified form. Inflows onto the central star clusters are triggered either by instabilities in the evolving pre-galactic disc and/or from mergers. Our aim was at comparing the efficiency of the GIRM channel with the already explored channels from Pop III (here reported as a reference) and from the collapse of supra-massive stars in young dense star clusters.

Our channel is active around redshift $z \sim 10-15$ as soon as the first NSCs form in the dark matter halos. Contrary to the two channels mentioned above, the GIRM is insensitive to the metallicity of the environment. The GIRM, by hypothesis, can occur in any star cluster that formed a core of ordinary stellar black holes, provided that (i) the star cluster is subjected to a massive inflow of gas which rises the central dispersion velocity above a given threshold, and that (ii) the stellar black holes present in the core had no time to be ejected by single-binary encounters prior the massive inflow. The lapse time between inflow events at the redshifts explored is $\lesssim 0.1$ Gyr. Black hole ejection in star clusters are seen to occur typically on times longer than ~ 1 Gyr (Downing et al. 2011), so that at early cosmic epochs this effect can be neglected. Conservatively, the results can be considered as upper limits.

We find that the GIRM channel is competitive, when compared to the channels studied in D09, D10 and D12 and can occur in concomitance with the formation of seeds from other channels, and in particular with that from runaway collisions of stars, in young dense clusters for which there is a partial overlap in the redshift space. We halt the simulation at $z \sim 6$, as our model to not account for the black hole growth due to accretion. Typically the black holes have seed masses in excess of $300 M_\odot$ with a mean of $\sim 1000 M_\odot$, opening the possibility that these black holes may later grow as supermassive at redshifts as early as $z \sim 7$, typical of the most distant QSOs.

These masses are in the range of the so-called intermediate mass black holes, which have not been yet observed in the Universe. If these black holes do not remain confined in galaxy centres but become wandering (like in the case of minor mergers of the host halo with a larger one), they could reach $z = 0$ without becoming massive black holes, and they could become potentially observable with their original mass.

There is no model yet that can describe the thermodynamics of a massive inflow of gas onto a pre-existing star cluster. The gas funnelled toward the centre of the cluster likely cools and fragment into stars, forming a more massive nuclear cluster nested into a primitive, lighter one. The key requirement of the DMB11 model, not proved to be realis-

tic yet, is a steepening of the gravitational potential such to lead to a major enhancement of the velocity dispersion inside the core of stellar mass black holes to trigger their relativistic collapse. Further modelling is necessary in this direction (Galanti et al. in preparation 2014).

ACKNOWLEDGMENTS

The authors are pleased to thank Jillian Bellovary, Melvin Davies, and Coleman Miller for a critical reading of the manuscript and their enlightening comments, and the Referee whose comments and queries helped improving the manuscript. MC and MV thank the Kavli Institute for Theoretical Physics at UC Santa Barbara for hospitality during progress on this work, while the program “A Universe of Black Holes” was taking place. MV acknowledges funding support from a Marie Curie Career Integration grant (PCIG10-GA-2011- 303609) within the framework FP7/PEOPLE/2012/CIG. This research was supported in part by the National Science Foundation under Grant No. NSF PHY11- 25915, through the Kavli Institute for Theoretical Physics and its program “A Universe of Black Holes”.

REFERENCES

- Abel T., Bryan G. L., Norman M. L., 2002, *Science*, 295, 93
- Agarwal B., Khochfar S., Johnson J. L., Neistein E., Dalla Vecchia C., Livio M., 2012, *MNRAS*, 425, 2854
- Barkana R., Loeb A., 2001, *Phys. Rep.*, 349, 125
- Begelman M. C., 2010, *MNRAS*, 402, 673
- Begelman M. C., Rossi E. M., Armitage P. J., 2008, *MNRAS*, 387, 1649
- Begelman M. C., Volonteri M., Rees M. J., 2006, *MNRAS*, 370, 289
- Bett P., Eke V., Frenk C. S., Jenkins A., Helly J., Navarro J., 2007, *MNRAS*, 376, 215
- Bromm V., Coppi P. S., Larson R. B., 2002, *ApJ*, 564, 23
- Bromm V., Loeb A., 2003, *ApJ*, 596, 34
- Callegari S., Kazantzidis S., Mayer L., Colpi M., Bellovary J. M., Quinn T., Wadsley J., 2011, *ApJ*, 729, 85
- Choi J.-H., Shlosman I., Begelman M. C., 2013, *ApJ*, 774, 149
- Ciotti L., Lanzoni B., Volonteri M., 2007, *ApJ*, 658, 65
- Clark P. C., Glover S. C. O., Klessen R. S., Bromm V., 2011, *ApJ*, 727, 110
- Davies M. B., Miller M. C., Bellovary J. M., 2011, *ApJ*, 740, L42
- Devecchi B., Volonteri M., 2009, *ApJ*, 694, 302
- Devecchi B., Volonteri M., Colpi M., Haardt F., 2010, *MNRAS*, 409, 1057
- Devecchi B., Volonteri M., Rossi E. M., Colpi M., Portegies Zwart S., 2012, *MNRAS*, 421, 1465
- Di Matteo T., Colberg J., Springel V., Hernquist L., Sijacki D., 2008, *ApJ*, 676, 33
- Dotan C., Rossi E. M., Shaviv N. J., 2011, *MNRAS*, 417, 3035
- Downing J. M. B., Benacquista M. J., Giersz M., Spurzem R., 2011, *MNRAS*, 416, 133

- Dunkley J., Komatsu E., Nolte M. R., Spergel D. N., Larson D., Hinshaw G., Page L., Bennett C. L., Gold B., Jarosik N., Weiland J. L., Halpern M., Hill R. S., Kogut A., Limon M., Meyer S. S., Tucker G. S., Wollack E., Wright E. L., 2009, *ApJS*, 180, 306
- Ferrara A., Haardt F., Salvaterra R., 2013, *MNRAS*, 434, 2600
- Glebbeek E., Gaburov E., de Mink S. E., Pols O. R., Portegies Zwart S. F., 2009, *A&A*, 497, 255
- Greif T. H., Springel V., White S. D. M., Glover S. C. O., Clark P. C., Smith R. J., Klessen R. S., Bromm V., 2011, *ApJ*, 737, 75
- Gürkan M. A., Freitag M., Rasio F. A., 2004, *ApJ*, 604, 632
- Haiman Z., Thoul A. A., Loeb A., 1996, *ApJ*, 464, 523
- Heger A., Fryer C. L., Woosley S. E., Langer N., Hartmann D. H., 2003, *ApJ*, 591, 288
- Koushiappas S. M., Bullock J. S., Dekel A., 2004, *MNRAS*, 354, 292
- Latif M. A., Schleicher D. R. G., Schmidt W., Niemeyer J. C., 2013, *MNRAS*, 436, 2989
- Lodato G., Natarajan P., 2006, *MNRAS*, 371, 1813
- Lodato G., Natarajan P., 2007, *MNRAS*, 377, L64
- Machacek M. E., Bryan G. L., Abel T., 2001, *ApJ*, 548, 509
- Madau P., Rees M. J., 2001, *ApJ*, 551, L27
- Mayer L., Kazantzidis S., Escala A., Callegari S., 2010, *Nature*, 466, 1082
- Merloni A., Heinz S., 2013, *Evolution of Active Galactic Nuclei*. Oswald, T. D. and Keel, W. C., p. 503
- Mihos J. C., Hernquist L., 1996, *ApJ*, 464, 641
- Miller M. C., Davies M. B., 2012, *ApJ*, 755, 81
- Monaco P., Theuns T., Taffoni G., 2002, *MNRAS*, 331, 587
- Montero P. J., Janka H.-T., Müller E., 2012, *ApJ*, 749, 37
- Moody K., Sigurdsson S., 2009, *ApJ*, 690, 1370
- Mortlock D. J., Warren S. J., Venemans B. P., Patel M., Hewett P. C., McMahon R. G., Simpson C., Theuns T., González-Solares E. A., Adamson A., Dye S., Hambly N. C., Hirst P., Irwin M. J., Kuiper E., Lawrence A., Röttgering H. J. A., 2011, *Nature*, 474, 616
- O’Leary R. M., Rasio F. A., Fregeau J. M., Ivanova N., O’Shaughnessy R., 2006, *ApJ*, 637, 937
- Omukai K., Palla F., 2001, *ApJ*, 561, L55
- Portegies Zwart S. F., McMillan S. L. W., 2002, *ApJ*, 576, 899
- Quinlan G. D., Shapiro S. L., 1987, *ApJ*, 321, 199
- Quinlan G. D., Shapiro S. L., 1989, *ApJ*, 343, 725
- Quinlan G. D., Shapiro S. L., 1990, *ApJ*, 356, 483
- Santoro F., Shull J. M., 2006, *ApJ*, 643, 26
- Strader J., Chomiuk L., Maccarone T. J., Miller-Jones J. C. A., Seth A. C., 2012, *Nature*, 490, 71
- Tegmark M., Silk J., Rees M. J., Blanchard A., Abel T., Palla F., 1997, *ApJ*, 474, 1
- Volonteri M., 2010, *A&A Rev.*, 18, 279
- Wise J. H., Turk M. J., Norman M. L., Abel T., 2012, *ApJ*, 745, 50
- Yoshida N., Omukai K., Hernquist L., 2008, *Science*, 321, 669